Co-published by
Institute of Fluid-Flow Machinery
Polish Academy of Sciences
Committee on Thermodynamics and Combustion
Polish Academy of Sciences

http://www.imp.gda.pl/archives-of-thermodynamics/

Numerical Studies on Symmetrically and Asymmetrically Heated Vertical Channels with Isothermal Walls

Chiyyedu Gururaja Rao

Department of Mechanical Engineering, Vasavi College of Engineering, Hyderabad, India
Author email: cgrr@staff.vce.ac.in, cgururajarao@gmail.com

Received: 12.06.2025; revised: 16.09.2025; accepted: 19.09.2025

Abstract

Numerical studies on combined free and forced convection together with radiation in a channel comprising two plates that are vertical and parallel are made. The channel here addresses two cases, viz. symmetric, and asymmetric isothermal walls. The cooling agent could be any gaseous medium that is assumed transparent to thermal radiation. The present work considers air for the job. The equations of conservation of mass, momentum and energy are solved through the finite volume method and an explicit code is prepared for this. The prime independent parameters considered are: aspect ratio, wall emissivity, Richardson number, Grashof number and Reynolds number. The effects exhibited by these parameters on the average convection Nusselt number, and the contributory roles enacted by convection and radiation in discarding the heat in the channel have been elucidated. The correlations for the mean convection Nusselt number and mean radiation Nusselt number are deduced through regression analysis using a large set of data gathered from the computer code that is prepared as part of the present work. The gross errors that occur in the cooling load calculations upon ignoring radiation in problems of this kind are clearly demonstrated.

Keywords: Vertical channel; Isothermal walls; Mixed convection; Radiation

Vol. 46(2025), No. 4, 135–140; doi: 10.24425/ather.2025.156844

Cite this manuscript as: Rao, C.G. (2025). Numerical Studies on Symmetrically and Asymmetrically Heated Vertical Channels with Isothermal Walls. *Archives of Thermodynamics*, 46(4), 135−140.

1. Introduction

Interaction of mixed (combined free and forced) convection with either (or both) of the other two modes of heat transfer, viz. conduction and radiation, continues to attract the attention of the researchers working in heat transfer. This is the case with all kinds of geometries (plates, channels, cavities, and so on). Carpenter et al. [1] reported their numerical studies on the role enacted by radiation along with developing laminar natural convection between vertical plates possessing asymmetric and uniform heat fluxes. Sparrow et al. [2] came out with their numerical calculations on coupled radiation and developing natural convection in a channel having one isothermal and one adiabatic wall. Anand et al. [3] performed numerical studies on the role exhibited by conduction and natural convection between asymmetrically heated plates subjected to uniform surface temperature. Almost simultaneously, Kim et al. [4] carried out numerical studies on a similar problem for the configuration of uniform surface heat flux. The governing equations were solved by them through the implicit finite difference method. Kim and Anand [5] performed a numerical study on developing laminar flow of a fluid and the accompanying transfer of heat between a string of parallel and conducting plates comprising the heat generating blocks mounted on their walls, with air taken as the coolant.

Nomenclature

A – aspect ratio of the vertical channel, [L/S]
$\overline{C_f}$ - mean friction coefficient
F_{ij} – view factor from the i^{th} to the j^{th} element of an enclosure
Gr_S – Grashof number, $(g\beta(T_L-T_\infty)S^3/\nu^2)$
g – local acceleration due to gravity, 9.81 m/s^2
G – irradiation, W/m^2
J – radiosity, W/m^2
L – channel height, m
$\overline{Nu}_C$(Left) – mean convection Nusselt number over the left wall, $-(1/A)\int_0^A(\partial\theta/\partial Y)_{Y=0}\,dX$
$\overline{Nu}_C$(Right) – mean convection Nusselt number over the right wall, $-(1/A)\int_0^A(\partial\theta/\partial Y)_{Y=1}\,dX$
$\overline{Nu}_C$ – mean convection Nusselt number over both walls, $\overline{Nu}_C$(Left)+$\overline{Nu}_C$(Right)
$\overline{Nu}_R$ – mean radiation Nusselt number over both walls, $\overline{Nu}_R$(Left)+$\overline{Nu}_R$(Right)
Pe_S- Peclet number based on channel spacing
Pr – Prandtl number, (ν/α)
Q – total rate of heat transfer from the channel, (Q_C+Q_R), W/m
Q_C – net convection heat transfer rate from the channel, W/m
Q_R – net radiation heat transfer rate from the channel, W/m
Re_S – Reynolds number, $[u_\infty S/\nu]$
Ri_S – Richardson number, $[Gr_S/Re_S^2]$
S – channel width (spacing), m
T – temperature at a given location, K
T_L – left wall temperature of the channel, K
T_R – right wall temperature of the channel, K
T_∞ – entry temperature of air, K
t – wall thickness, m
U, V – non-dimensional vertical and horizontal velocities
u_∞ – entry velocity of air, m/s
x, y – axial and transverse distances, respectively, m
X, Y – normalised axial and normalised transverse distances, [x/S] and [y/S], respectively

Greek symbols

ε – channel wall emissivity
θ – normalised local temperature, $[(T-T_\infty)/(T_L-T_\infty)]$
σ – Stefan-Boltzmann constant, 5.6697×10^{-8} W/(m^2 K^4)
ψ,ω – non-dimensional stream and vorticity functions

Hacohen et al. [6] documented experimental as well as numerical findings on the formation of the boundary layer together with heat transfer coefficients in several thermally simulated electronic components catering to both forced and free convection environments in a channel. Watson et al. [7] worked on numerical simulations on laminar combined natural and forced convection between several plates that are parallel and vertically disposed, carrying planar heating elements.

Gururaja Rao [8] explored coupled conduction-mixed convection-radiation from the configuration of a plate that is vertically disposed and has an embedded discrete heater that traverses along the plate, and elucidated, quantitatively as well as qualitatively, the roles enacted by the two surface heat transfer modes, viz. convection and radiation. Multi-mode heat transfer connecting free convection and internal thermal conduction speaking about a vertical heat generating plate has been probed by Mamun et al. [9]. A theoretical investigation narrating mixed convection flow of a nanofluid consisting of water and alumina for the geometry of a vertical micro channel has been credited to Malavandi and Ganji [10]. Londhe and Gururaja Rao [11] delved into the interplay between combined natural and forced convection, conduction and radiation catering to a channel held vertically and heated discretely. They handled the channel that had three identical and symmetrically positioned embedded discrete heaters in the left wall of the channel. Fairly recently, Shah and Gururaja Rao [12] extended the above work by replacing the identical and symmetrically positioned heaters with five discrete heaters of progressively decreasing sizes in the left wall of the channel. The results of a conjugate study on heat transfer by the combined modes of natural convection and radiation from an array of fins have been documented by de Araujo et al. [13], making use of a semitransparent fluid medium as the cooling agent.

A review of the various findings documented in multi-mode heat transfer from the geometry of a channel indicated that a detailed probe into the channel geometry that comprises (i) symmetrically and (ii) asymmetrically heated isothermal walls is not explicitly covered in the literature. Thus, the same has been explored in the current paper. The finite volume method (FVM) is used for this purpose. It is also proposed to prepare an appropriate computer program to tackle the present problem. Along with the simulation studies, an attempt is made here to arrive at the correlations for (i) mean convection Nusselt number and (ii) mean radiation Nusselt number through a huge numerical data set obtained from the computer code written here.

2. Problem description and solution methodology

Figure 1 shows the vertical parallel wall channel of height L and spacing (or width) S.

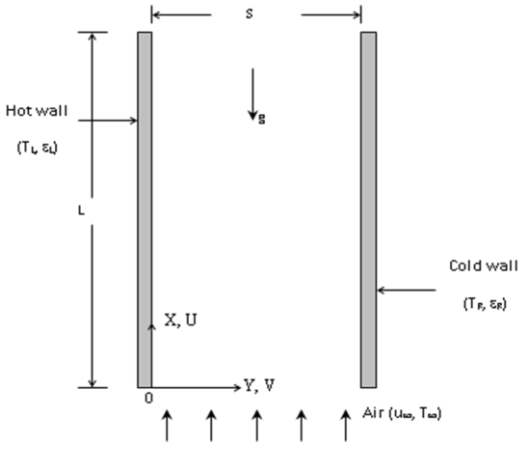

Fig. 1. Symmetrically or asymmetrically heated vertical channel considered in the present study.

The aspect ratio (A) of the channel is defined as (L/S). For a given height (L), a larger A implies a narrower channel, and a smaller A pertains to a broader channel. The left wall is hotter (T_L) than the right wall (T_R) for the case of "asymmetric wall heating", while both walls acquire identical temperatures

($T_R = T_L$) for the case of "symmetric wall heating". The left and right wall emissivities are, respectively, ε_L and ε_R, and these too may (or may not) be equal. The cooling agent (air) is seen entering the channel from the bottom end at a uniform velocity [u_∞] and a uniform temperature [T_∞]. The basic equations of conservation of mass, momentum, and energy, after their initial conversion into vorticity-stream function form and an accompanying normalisation, are:

$$U\frac{\partial\omega}{\partial X}+V\frac{\partial\omega}{\partial Y}=-\mathrm{Ri}_S\frac{\partial\theta}{\partial Y}+\frac{1}{\mathrm{Re}_S}\left[\frac{\partial^2\omega}{\partial X^2}+\frac{\partial^2\omega}{\partial Y^2}\right], \quad (1)$$

$$\frac{\partial^2\psi}{\partial X^2}+\frac{\partial^2\psi}{\partial Y^2}=-\omega, \quad (2)$$

$$U\frac{\partial\theta}{\partial X}+V\frac{\partial\theta}{\partial Y}=\frac{1}{\mathrm{Pe}_S}\left[\frac{\partial^2\theta}{\partial X^2}+\frac{\partial^2\theta}{\partial Y^2}\right]. \quad (3)$$

The Richardson number (Ri_S), based on the channel spacing (S), and defined as ($\mathrm{Gr}_S/\mathrm{Re}_S^2$), appears in the vorticity-transport equation (Eq. (1)). It marks the distinction between different regimes of convection, viz. forced convection dominant ($\mathrm{Ri}_S << 1$), pure mixed convection ($\mathrm{Ri}_S = 1$) and free convection dominant ($\mathrm{Ri}_S >> 1$) regimes. The "enclosure method of analysis" comprising the radiosity (J) – irradiation (G) formulation is used for the calculations involving radiation.

2.1. Boundary conditions used

The various boundary conditions used in the current study are shown in Fig. 2.

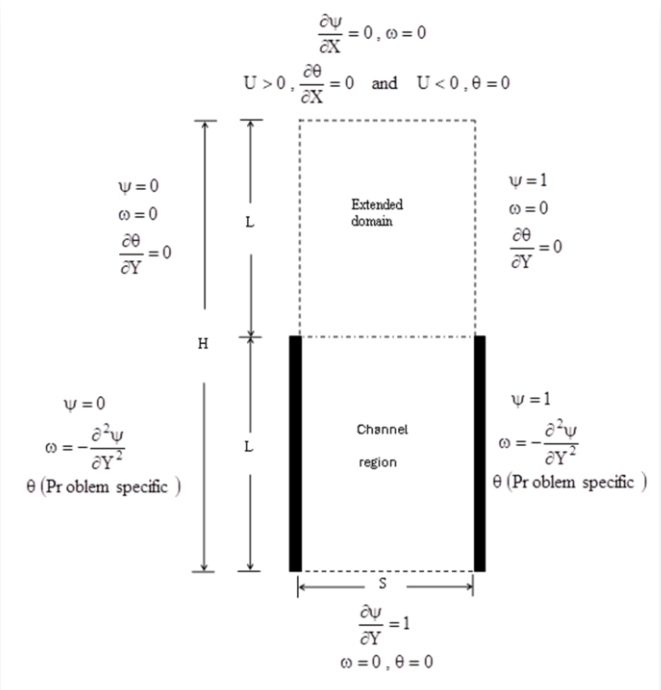

Fig. 2. Various boundary conditions used in the present study.

2.2. Discretisation of the computational domain and the grid sensitivity test

The computational domain has been discretised adhering to the condition that a specific number of finer grids always exist (i) at the bottom end of the channel from where the fluid (air) begins its flow and (ii) near each channel wall, where the gradients of velocity and temperature are comparatively steeper. This led to using the "cosine function" to generate the grids in Y-direction, and a "semi-cosine function" is used in X-direction along the channel walls. In the domain beyond the channel exit, uniformly spaced grids are preferred in axial direction, without any change in the grid pattern in Y-direction.

A "grid sensitivity test" is conducted for a typical case with $T_L = T_R = 100^oC$, $A = 8$, $\mathrm{Ri}_S = 1$, $\mathrm{Re}_S = 100$ and $\mathrm{Gr}_S = 10000$. The grid sensitivity is tested in two stages – first with M fixed and later with N fixed. The results of the first stage show that the difference in $\overline{\mathrm{Nu}}_C$ between the grid sizes 81×141 and 81×161 is 0.008%, while the difference in $\overline{C}_f$ between the same two grid sizes is 0.0002%. The results of the second stage of the study with N fixed indicate that the difference in $\overline{\mathrm{Nu}}_C$ between grid sizes 81×141 and 101×141 is 0.72%, while for $\overline{C}_f$, the difference between these two grid sizes is 0.55%. In view of these results, M and N have been fixed as 81 and 141, respectively.

It is to be noted that, in the above study, the number of grid elements along the channel is 90 (i.e. the number of nodes along the channel $N_1 = 91$), which is based on another study for the same typical case as above. It can be noticed from the table that the difference in $\overline{\mathrm{Nu}}_C$ between $N_1 = 71$ and 91 is 4.39%, while that between $N_1 = 91$ and 111 is 0.51%. Regarding $\overline{C}_f$, the difference between $N_1 = 71$ and 91 is 0.083% and that between $N_1 = 91$ and 111 is 0.029%. Thus, N_1 is fixed as 91. Hence, for all the subsequent calculations, a grid pattern with $M = 81$, $N_1 = 91$ and $N = 141$ is used. Figure 3 illustrates one such typical grid system used in the current work.

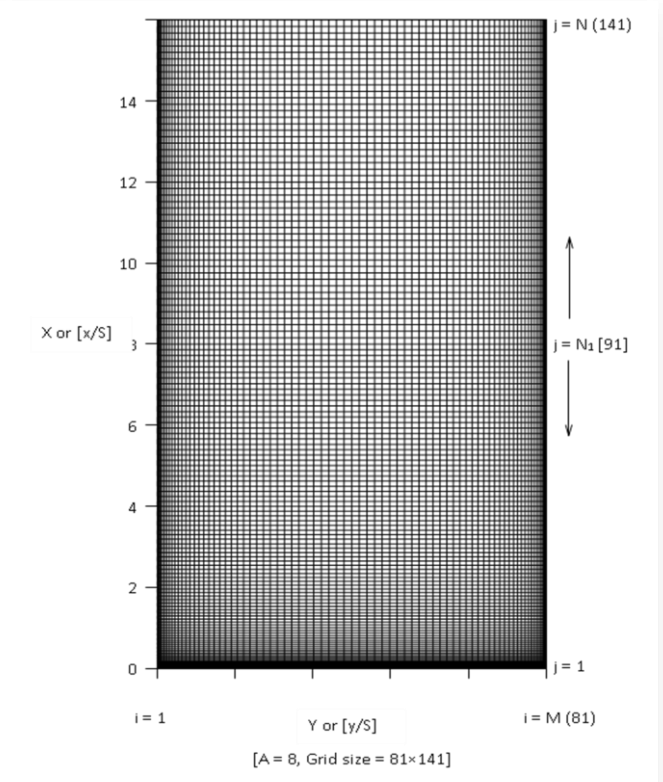

Fig. 3. Grid pattern used for one of the cases of the present work.

2.3. Calculations

The velocities and temperatures everywhere in the computational domain are the initial results in the work. The local convection Nusselt numbers along the two walls (both hot and cold) are evaluated by using a second degree Lagrangian polynomial, while the mean convection Nusselt number ($\overline{Nu}_C$) based on each of the two walls is calculated by numerical integration (the Simpson's 1/3 rule). The mean convection Nusselt number based on both walls ($\overline{Nu}_C$) is then obtained by adding algebraically the mean convection Nusselt numbers based on each channel wall, thus calculated. On similar lines, the mean radiation Nusselt number ($\overline{Nu}_R$) based on both walls is the algebraic sum of the mean radiation Nusselt numbers on the two walls. All the calculations are made employing air (cooling agent) that is treated as non-participating in radiation. The height (L) of the channel is taken equal to 23.34 cm.

3. Results and discussion

In this section, some prominent results obtained in the present study will be presented.

3.1. Dependence of mean convection Nusselt number on other parameters

Figure 4 shows a family of curves depicting variations of the average convection Nusselt number ($\overline{Nu}_C$) with Richardson number (Ri_S). The curves are plotted for four values of aspect ratio (A = 4, 8, 12 and 16) for a typical case of symmetric wall heating (θ_R = 1), with $T_L = T_R$ = 100°C.

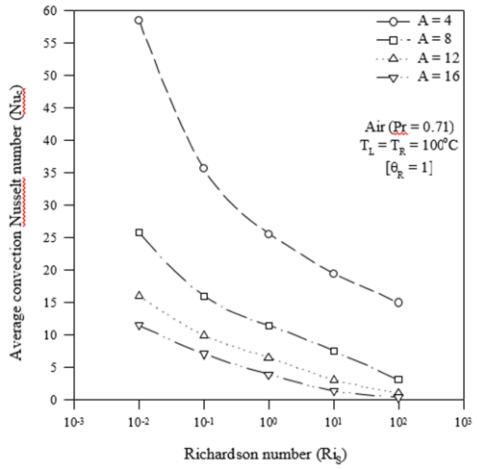

Fig. 4. Dependence of mean convention Nusselt number on Richardson number for different aspect ratios of the channel.

The figure reveals that, for a given aspect ratio (A), $\overline{Nu}_C$ decreases as Ri_S increases from 0.01 to 100. This is because, in this example, Gr_S is held fixed, and thus Re_S decreases as Ri_S increases. This means that the flow shifts from the regime of forced convection to that of natural convection, which brings down the heat transfer rate and thus the Nusselt number in the channel. However, the amount of decrease in $\overline{Nu}_C$ is higher in the forced convection regime ($0.01 \le Ri_S < 1$) than in the natural convection regime ($1 < Ri_S \le 100$). Calculations indicate that, for A = 4, $\overline{Nu}_C$ decreases by 55% between Ri_S = 0.01 and 1, while it decreases only by about 34% between Ri_S = 1 and 100. Also, beyond Ri_S = 100, the variation in $\overline{Nu}_C$ tends to be asymptotic with reference to Ri_S, especially towards larger aspect ratios. The figure further indicates that $\overline{Nu}_C$ diminishes as the aspect ratio (A) increases between 4 and 16, for a given Ri_S. This is because, with the channel height (L) remaining unaltered as A increases, the channel spacing (S) decreases. Since $\overline{Nu}_C$ is based on S, there is an understandable decrease in $\overline{Nu}_C$ with the increasing A. Looking into the example here, for Ri_S = 1 (mixed convection), $\overline{Nu}_C$ is found to decrease by as much as 84% as the aspect ratio increases from 4 to 16. Trends of a similar kind are perceived in the case of asymmetric wall heating also.

3.2. Roles taken up by convection and radiation in channel heat dissipation

In the current problem, both convection and radiation contribute to dissipation of heat from the channel. The heat transferred by convection (free and forced) and that transferred by radiation are independently calculated. The net heat transfer in the channel is then obtained as the algebraic sum of the rates of convection and radiation heat transfer. The design of any cooling system (e.g. for electronic equipment) that uses a gaseous medium (say air) as the coolant should necessarily take radiation into account, because a sizable amount of heat may get transferred by radiation in all such applications. The current study is taken up to address this issue adequately.

The role radiation plays in heat transfer from the channel can be best delineated by considering a typical case with A = 4, $T_L = T_R$ = 100°C (θ_R = 1), T_∞ = 25°C and $Gr_S = 10^4$. Five values of Ri_S (= 0.01, 0.1, 1, 10 and 100) and three values of wall emissivity ($\varepsilon_L = \varepsilon_R$ = 0.05, 0.45 and 0.85) are considered. In this study, convection heat transfer is not a function of emissivity (ε), while radiation heat transfer is not a function of Richardson number (Ri_S). Figure 5 shows a family of curves depicting the relative roles enacted by convection and radiation in channel heat dissipation plotted against Ri_S for the three values of emissivity opted above.

It is noticeable that the role exhibited by convection tapers down as Ri_S increases from 0.01 to 100 for a given ε, while the contribution of radiation continuously increases. In the example here, for ε = 0.45, the radiation heat transfer (Q_R) remains constant at 126.54 W/m for all values of Ri_S. However, the convection heat transfer (Q_C) decreases from 313.99 W/m to 60.35 W/m, as Ri_S increases from 0.01 to 100. The net result is that the total heat transfer (Q) decreases from 440.53 W/m to 186.89 W/m. Thus, the convection contribution in the total heat transfer decreases from 71.28% to 32.29%, with a mirror-image increment in radiation heat transfer from 28.72% to 67.71%. If one were to design a cooling system overlooking radiation, the heat dissipation rate in the channel for Ri_S=100 would have been reported as only 60.35 W/m (= Q_C). However, there is an accompanying radiation heat transfer of 126.54 W/m (for $\varepsilon_L = \varepsilon_R$ = 0.45), which is more than two times the convection heat transfer rate.

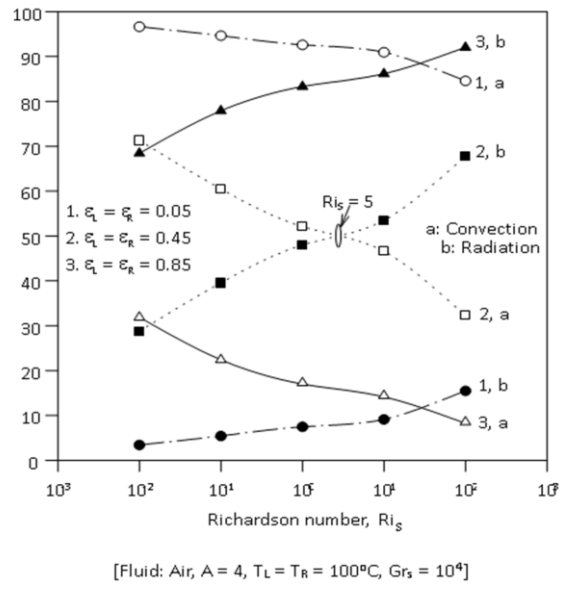

Fig. 5. Contributory roles enacted by convention and radiation in heat transfer.

It can also be noticed that the curves belonging to convection and radiation cross each other for the case where $\varepsilon_L = \varepsilon_R = 0.45$, implying equal contributions to heat transfer at $Ri_S \approx 5$. The figure also reveals that for a given Ri_S, there is a continuous decrease in the percentage of convection heat transfer, with a proportionate increase in its radiation counterpart, as ε (ε_L or ε_R, which are equal in this specific example) increases from 0.05 to 0.85. In the current example, for $Ri_S = 1$, the heat transfer by convection (Q_C) remains constant at 137.3 W/m for all values of ε (due to its non-dependence on ε). The radiation heat transfer (Q_R), on the other hand, increases from 11.03 W/m to 671.32 W/m, as ε increases from 0.05 to 0.85. In effect, the share of convection in total heat transfer drops down from 92.56% to 16.9%, with the contribution from radiation increasing from 7.44% to 83.1%. In this context, if a cooling system is designed ignoring radiation, and if the channel walls, for example, have an emissivity (ε) of 0.85, the heat transfer rate would have been calculated as 137.3 W/m (= Q_C) only. However, the radiation heat transfer for this case is 671.32 W/m. Thus, there is a total heat transfer of 808.62 W/m here, which is about 5.9 times the heat transfer (Q_C) that would have been reported had radiation been ignored. The above exercise thus highlights the importance of the role radiation plays in this class of problems.

3.3. Correlations for the case of symmetric wall heating

The following ranges of different independent parameters have been used here:

$$1 \le A \le 16,$$
$$0.05 \le \varepsilon_L, \quad \varepsilon_R \le 0.85,$$
$$0 \le \theta_R \le 1,$$
$$0 < T_{R_1} \le 1,$$
$$0 < T_{R_2} \le 1,$$
$$0.01 \le Ri_S \le 100,$$
$$1 \le Re_S \le 10000,$$
$$10 \le Gr_S \le 10000.$$

A correlation has been deduced for the mean convection Nusselt number ($\overline{Nu}_C$) based on both walls of the channel:

$$\overline{Nu}_C = 2.84\, A^{-0.65} T_{R_1}^{0.49}\, Re_S^{0.46}\, (1 + Ri_S)^{0.09}. \qquad (4)$$

It is to be noted that $\overline{Nu}_C$, correlated above, is based on the channel spacing (S). Equation (4) has the coefficient of correlation equal to 0.991 and the error band equal to $\pm$ 4.3%. For obtaining the correlation above, $(1+Ri_S)$ has been chosen as the most appropriate form for Ri_S. This is due to the reason that, in the situation where $Ri_S = 0$, $\overline{Nu}_C$ would not be zero since it still possesses the forced convection component.

For the left wall of the channel, based on a set of 45 data points, a correlation for $\overline{Nu}_R$ turns out to be:

$$\overline{Nu}_R(\text{Left}) = 187.46\, A^{-1.12}(1 - T_{R_1}^4)^{-0.09} \varepsilon_L^{1.55} \varepsilon_R^{-0.07}. \qquad (5)$$

The coefficient of correlation given by Eq. (5) is 0.998, and it has the error band = $\pm$ 4.9%. For the same 45 data points as used for Eq. (5), the correlation for $\overline{Nu}_R$, based on the right wall of the channel, having the coefficient of correlation equal to 0.993 and the error band equal to $\pm$ 5.1%, turned out to be:

$$\overline{Nu}_R(\text{Right}) = 171.89\, A^{-1.18}(1 - T_{R_1}^4)^{-0.49}\, \varepsilon_L^{0.03} \varepsilon_R^{1.64}. \qquad (6)$$

3.4. Correlations for the case of asymmetric wall heating

The mean convection Nusselt number ($\overline{Nu}_C$) based on both channel walls (left as well as right), for asymmetric wall heating, has been correlated, using 151 data points, as:

$$\overline{Nu}_C = 1.72\, A^{-0.71}(1 + \theta_R)^{0.77} Re_S^{0.45} (1 + Ri_S)^{0.08}. \qquad (7)$$

Equation (7) has the coefficient of correlation equal to 0.993 and the error band equal to $\pm$ 4.8%. The form $(1+\theta_R)$ has been chosen to be appropriate for θ_R, because θ_R varies from 0 to 1, and $\overline{Nu}_C$ would be finite even when $\theta_R = 0$. The form $(1+Ri_S)$ is retained for Ri_S following the reasons already explained.

The correlation for $\overline{Nu}_R$, based on the left (hot) wall, evolved using 116 data that has the coefficient of correlation equal to 0.996 and the error band equal to $\pm$ 5.6%, is:

$$\overline{Nu}_R(\text{Left}) = 48.52\, A^{-1.16}(1 - T_{R_1}^4)^{-2.75} \times \times (1 - T_{R_2}^4)^{-0.02}\, \varepsilon_L^{1.59} \varepsilon_R^{-0.02}. \qquad (8)$$

The correlation for $\overline{Nu}_R$ for the right (cold) wall, based on 105 data points and having the coefficient of correlation equal to 0.995 and the error band equal to $\pm$ 5.7%, is:

$$\overline{Nu}_R(\text{Right}) = 1.77\, A^{-0.82}(1 - T_{R_1}^4)^{-2.77} \times \times (1 - T_{R_2}^4)^{-1.36}\, \varepsilon_L^{-0.39} \varepsilon_R^{1.57}. \qquad (9)$$

In the above correlations for $\overline{Nu}_R$, $(1 - T_{R_1}^4)$ and $(1 - T_{R_2}^4)$ have been chosen to be the appropriate forms for the two temperature ratios T_{R_1} (= T_∞/T_L) and T_{R_2} (= T_R/T_L), respectively.

4. Conclusions

Some of the prominent conclusions derivable from the current numerical study include:

- The aspect ratio (A) plays a prominent role in the current problem. An increasing aspect ratio, and thus the progressively narrower channels, are found to bring down the mean convection Nusselt number ($\overline{\mathrm{Nu}}_\mathrm{C}$). This happens in all regimes of mixed convection. For example, in the pure mixed convection regime (Ri_S = 1), $\overline{\mathrm{Nu}}_\mathrm{C}$ decreases by a maximum of about 80 – 85% (depending on other parameters) with the aspect ratio rising from 4 to 16.
- For a given aspect ratio (A), $\overline{\mathrm{Nu}}_\mathrm{C}$ generally decreases with Ri_S. This trend is found to be more apparent in the region of forced convection dominance (viz. $0.01 \leq \mathrm{Ri}_S < 1$) as against the region of free convection dominance (viz., $1 < \mathrm{Ri}_S \leq 100$).
- The fact that the heat load calculation in any application that makes use of a gaseous medium (like air) as the coolant turns out to be erroneous if one does not take radiation into account has been adequately established. A detailed graphical narration has been given in this context.
- Correlations for the mean convection Nusselt number ($\overline{\mathrm{Nu}}_\mathrm{C}$) and mean radiation Nusselt number ($\overline{\mathrm{Nu}}_\mathrm{R}$) evolved making use of a very large number of data points obtained using the computer program exclusively written in the current work.

References

[1] Carpenter, J.R., Briggs, D.G., & Sernas, V. (1976). Combined radiation and developing laminar free convection between vertical flat plates with asymmetric heating. *ASME Journal of Heat Transfer*, 98(1), 95−100. doi: 10.1115/1.3450476

[2] Sparrow, E.M., Shah, S., & Prakash, C. (1980). Natural convection in a vertical channel: 1. Interacting convection and radiation; 2. The vertical plate with and without shrouding. *Numerical Heat Transfer*, 3(3), 297−314. doi: 10.1080/01495728008961760

[3] Anand, N.K., Kim, S.H., & Aung, W.(1990). Effect of wall conduction on free convection between asymmetrically heated vertical plates: uniform wall temperature. *International Journal of Heat and Mass Transfer*, 33(5), 1025−1028. doi: 10.1016/0017-9310(90)90083-7

[4] Kim, S.H., Anand, N.K., & Aung, W. (1990). Effect of wall conduction on free convection between asymmetrically heated vertical plates: uniform wall heat flux. *International Journal of Heat and Mass* Transfer, 33(5), 1013−1023. doi: 10.1016/0017-9310(90)90082-6

[5] Kim, S.H., & Anand, N.K.(1994). Laminar developing flow and heat transfer between a series of parallel plates with surface-mounted discrete heat sources. *International Journal of Heat and Mass Transfer*, 37(15), 2231−2244. doi: 10.1016/0017-9310(94)90366-2

[6] Hacohen, J., Chiu, T.W., & Wragg, A.A. (1995). Forced and free convective heat transfer coefficients for a model printed circuit board channel geometry. *Experimental Thermal and Fluid Science*, 10(3), 327−334. doi: 10.1016/0894-1777(94)00073-H

[7] Watson, J.C., Anand, N.K., & Fletcher, L.S. (1996). Mixed convective heat transfer between a series of vertical parallel plates with planar heat sources. *ASME Journal of Heat Transfer*, 118(4), 984−990. doi: 10.1115/1.2822601

[8] Gururaja Rao, C. (2004). Buoyancy-aided mixed convection with conduction and surface radiation from a vertical electronic board with a traversable discrete heat source. *Numerical Heat Transfer, Part A: Applications*, 45(9), 935−956. doi: 10.1080/10407780490439202

[9] Mamun, A.A., Chowdhury, Z.R, Azim, M.A, & Maleque, M.A. (2008). Conjugate heat transfer for a vertical flat plate with heat generation effect. *Nonlinear Analysis: Modelling and Control*, 13(2), 213−223. doi: 10.15388/NA.2008.13.2.14581

[10] Malvandi, A.,& Ganji, D.D. (2014).Mixed convective heat transfer of water/alumina nano fluid inside a vertical microchannel. *Powder Technology*, 263, 37−44. doi: 10.1016/j.powtec.2014.04.084

[11] Londhe, S.D. & Gururaja Rao, C. (2014). Interaction of surface radiation with conjugate mixed convection from a vertical channel with multiple discrete heat sources. *Heat and Mass Transfer*, 50, 1275–1290. doi: 10.1007/s00231-014-1333-1

[12] Shah A.P., & Gururaja Rao, C. (2020). Buoyancy-aided conjugate mixed convection with surface radiation from a vertical channel with multiple non-identical discrete heat sources. *International Journal for Computational Methods in Engineering Science and Mechanics*, 21(1), 12−25. doi: 10.1080/15502287.2020.1718799

[13] de Araujo, M.E.V., Barbosa, E.G., Martins, M.A., & Corrêa, P.C. (2022). Conjugated analysis of heat transfer by natural convection and radiation in a fin array using a semitransparent fluid medium. *Heat and Mass Transfer*, 58, 1119−1132. doi: 10.1007/s00231-021-03163-1